Novel Acridine Orange Staining Protocol and Microscopy with UV Surface Excitation Allows for Rapid Histological Assessment of Canine Cutaneous Mast Cell Tumors

Croix Griffin[1], Richard Levenson[2], Farzad Feredouni[2], Austin Todd[2]

1. School of Veterinary Medicine, University of California, Davis 2. Department of Pathology and Laboratory Medicine, University of California, Davis

Introduction

- Mast cell tumors (MCTs) represent up to 27% of all malignant cutaneous tumors in dogs. Diagnosis is easily made with cytology, however the grade of the tumor determines prognosis and required margins.[1]
- Grade is not typically known until at least 48 hours after the surgery, as pre-surgical incisional biopsies are impractical due to additional cost and risk to the patient.
- Up to 30% of all mid to high grade mast cell tumors recur when incompletely excised. Recurrence is correlated with progression to malignancy in 59% of patients.[2]
- Low grade tumors are unlikely to recur regardless of margin cleanliness.[3] When removed with wide margins, the patient endures unnecessary short term morbidity from a 'surgical overdose'.
- MCTs commonly occur in areas such as the face, perineum, and distal limbs where excision with the standard recommended margins are not feasible.
- Very recent attempts to solve this margin assessment problem have been unsuccessful (impression cytology, 2017[4]) or even potentially dangerous for the patient (in-vivo fluorescent probe detection, 2016[5]).

Hypothesis

A novel Acridine Orange (AO) tissue staining protocol for MUSE, once optimized, accurately highlights mast cells and the most critical histologic features of mast cell tumors in fresh, thick tissue slices.

Materials & Methods

- Fixed tissue from 7 MCTs (Kiupel[6] grades; 2 high, 5 low) and fresh tissue from one low grade MCT were obtained from the UC Davis VMTH pathology service. Slides from the above tissues as well as from various other 'look-a-like' round cell tumors stained and analyzed.
- The new protocol (**Fig. 3**) is a significant modification of the Zachrisson (1967)[7] method for fluorescence microscopy. Images were analyzed with free, open-source software QuPath[8] and ImageJ[9]. Statistical analyses were performed in R. Data analysis was mostly restricted to slides and tissue from the MCT removed on July 27th as formalin fixation significantly impaired stain performance.
- Correlation between thick tissue and slide staining (**Figs. 6, 7**) will be measured by comparing overall % area stained of large regions and with a comparison of average difference in hue between MC nucleus and cytoplasm. An RGB spectral phasor (www.spechron.com) will be used to remove the background signal.
- AO stained slides were first imaged with the MUSE microscope (**Fig. 7**), next completely destained with 40% methanol and 10% glacial acetic acid, then re-stained with 0.1% Toluidine Blue (TB) at pH 2.20 and 0.01% Eosin counterstain (**Fig. 8**). Slides were scanned with a Leica digital scanner at 40X and compared on a region (ROI) to region (ROI) and cell to cell basis.
- 14 AO Thin MUSE and corresponding TB ROI tiles containing a mixture of tumor and nontumor cells were selected semi-randomly, assigned a random identifier, and flipped or rotated to provide blinding during analysis. These ROI's included approximately 380 total mast cells.
- Color thresholding with fixed ranges (generated with an independent consultant) measured the positively stained (purple or orange) pixels (**Figs. 7b, 8b**), the combined area of which was assessed as a percentage of the ROI. Percent areas stained were assessed with a Bland-Altman 97.5% limits of agreement and a 95% CI (Wilcoxon Signed-Rank test) around the median difference in percent area stained.
- Stain agreement regarding the number of mast cells in a given ROI was assessed with a Wilcoxon Signed-Rank test for the blinded cell counts of the primary author across the 14 paired ROIs as well as the blinded median cell counts provided by 7 additional people not affiliated with the project.
- Detectability of the AO stained mast cells in the thick tissue by a machine learning algorithm will be quantified in fresh thick tissue ROIs containing tumor and nontumor areas. Thus far, a random trees classifier has only required an average of about 500 training objects to identify mast cells appropriately.
- 1268 low grade mast cells and 1194 high grade mast cells were measured for nuclear circularity and eccentricity and sampled in an attempt to assess nuclear pleomorphism, however, hypothesis testing failed to find any significant differences between high and low grade cells.
- To quantify the correlation between AO fluorescence signal intensity and the granularity of a given cell, saturation intensity (mean grey value, HSB stack slice 2) of the thresholded cytoplasm from individual mast cells will be compared as a percentage of the saturation intensity of a common baseline, heavily stained cell for both stains. These findings will be interpreted alongside rating scale scores (1-5) of staining intensity of the individual cells from the surveyed outside evaluators.

Figure 1. Example of MCT removal surgery. Single or multiple biopsies can be cut by hand from the tumor bed or tumor itself.

Figure 2. Blue arrow route does not require formalin fixation or thin sectioning. Slice is approx. 5 x 4 x 2 mm.

- Stained for 1 minute with 0.03% Acridine Orange titrated to pH 0.53 with HCl
- Rinsed in phosphate buffered saline for 1 minute at 50°C

Figure 3. A streamlined, robust, yet relatively gentle MC staining protocol was developed.

Figure 4. MUSE Microscope. Please visit www.musepathology.com for more information about the new technology.

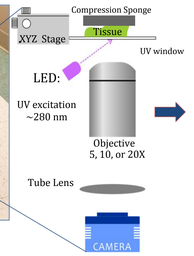

Figure 5. Optical setup.

- Standard histology processing, 3-5 µm section on a slide

Toluidine Blue (control)

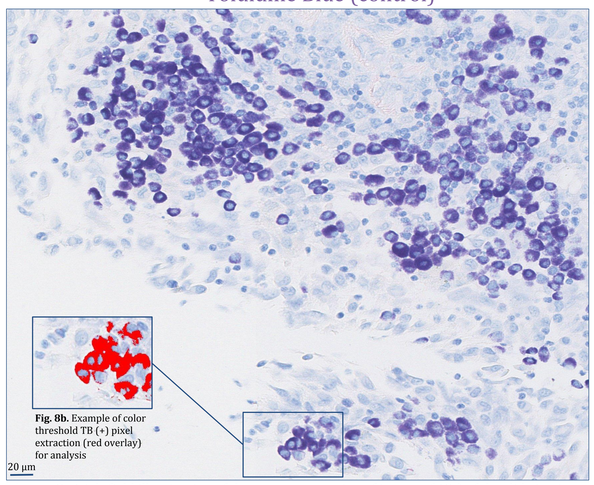

Fig. 8b. Example of color threshold TB (+) pixel extraction (red overlay) for analysis

Slide destained, then restained

Acridine Orange (novel protocol)

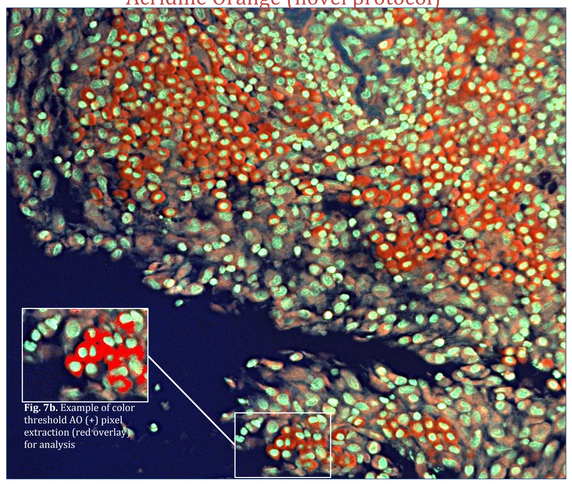

Fig. 7b. Example of color threshold AO (+) pixel extraction (red overlay) for analysis

Figure 8. Brightfield illumination of the exact same region of interest (ROI) of the slide in Fig. 7 after destaining and then restaining with Toluidine Blue (TB). The two stains appear to agree regarding the location and relative intensity of each MC. [40X]

Figure 7. "Thin MUSE" generated region of interest (ROI) from the same tumor shown in Fig. 6. To ensure staining activity in these 3-5 µm sections was representative of the staining activity seen in the thick tissue, the slides were stained with the exact same protocol (**Fig. 3**.) [20X]

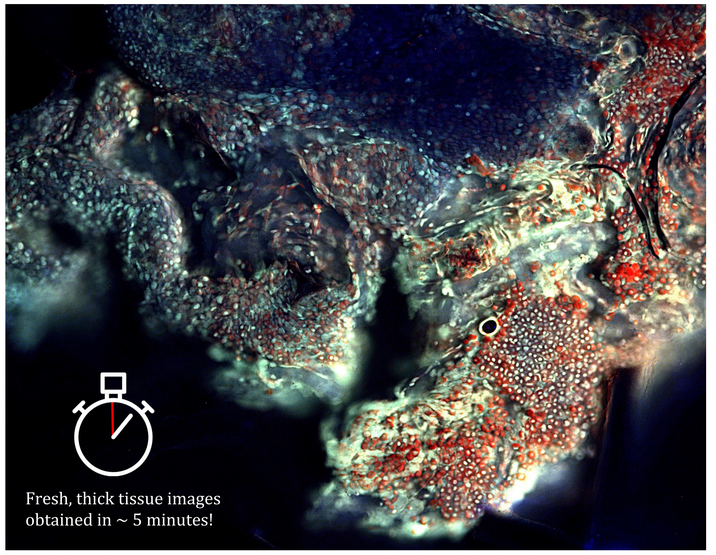

Figure 6. Fresh tissue from the center of a Kiupel low grade MCT stained with Acridine Orange (**Fig. 3**). Mast cells are stained metachromatically with green nuclei and red/orange cytoplasm. Stromal and other inflammatory cells do not have a red cytoplasm. Entire region is positive for mastocytosis; however, tissue on the left side of the image contains fewer mast cells. This image demonstrates 2.5 D surface architecture, but entire field can be brought into focus with swept focus averaging and extended depth of field software adjustments if desired. Objective: 10X.

Results

- AO and TB strongly agreed regarding the percentage of area stained (thresholded) across 14 paired ROI's. The median difference between the percentage area stained was just 0.94% and a Wilcoxon Signed-Rank test found a 95% CI of [0.147, 2.71]. The Bland-Altman 97.5% limit of agreement was 5.62% (**Fig. 10**).
- Cell counts across the 14 paired ROI's matched fairly well but not perfectly. The author's counts and the median counts of the seven outside evaluators had median differences (and Wilcoxon 95% CIs) across the paired ROIs of 8 cells [3.99, 13.0] and 7.5 cells [1.75, 10.49] respectively. B-A 97.5% limits of agreement were 22.7 cells and 25.1 cells, respectively. Count differences were most likely due to confusion over processing artifacts.

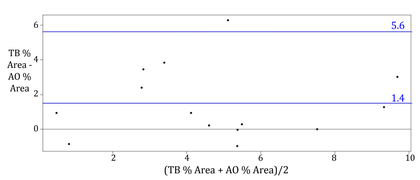

Figure 10. Bland-Altman Plot with 2.5% and 97.5% limits of agreement for the the Acridine Orange and Toluidine Blue color thresholded percentage of area stained over 14 ROIs comprising 495 mm² of slide mounted tissue.

Key Findings

- Metachromasia of Acridine Orange is the result of ionized dye aggregates inside the low pH cytoplasmic vacuoles of mast cells which fluoresce at 630 nm (orange). This is consistently apparent with 280 nm excitation and allows clear distinction between MC nuclei, MC cytoplasm, and background.
- Negative control slides from 6 different dermal round cell tumors did not feature the bright orange cytoplasmic staining of MCs but some did fluoresce with a (potentially useful) lighter orange or peach color (**Fig. 11**).
- Two high grade MCT's had distinctive morphological features seen in thick tissue. One was extremely cellular and the other was highly infiltrative of healthy tissue with clusters of MCs (**Fig. 12**).
- Higher magnification and better resolution are needed to reliably detect mitotic figures or visualize chromatin detail.

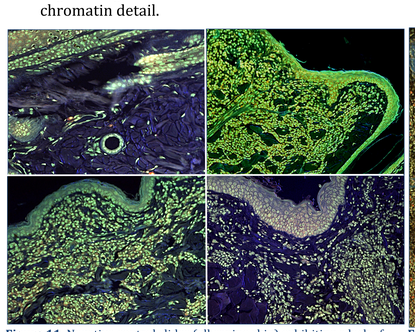

Figure 11. Negative control slides (all canine skin) exhibiting a lack of bright red-orange cytoplasmic staining after applying the protocol in Fig. 3. Clockwise starting top left: Normal skin and hair follicle with two mast cells, histiocytoma, cutaneous lymphoma, plasmacytoma. [20X]

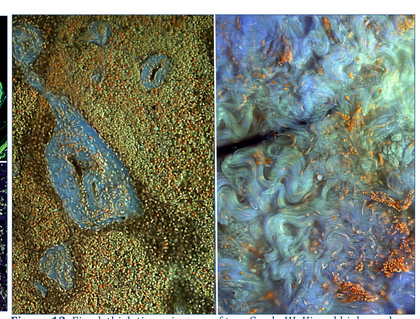

Figure 12. Fixed, thick tissue images of two Grade III, Kiupel high-grade MCTs. Both have distinctive morphology. Tumor on the left was inflamed and extremely cellular. Tumor on the right was comprised of packets of mast cells that infiltrated healthy connective tissue. [10X]

Conclusions & Future Aims

- The simple and fast Acridine Orange staining method developed in this study reliably highlights mast cells and distinguishes them from other inflammatory cells.
- The stain is highly agreeable with Toluidine Blue. Ongoing statistical evaluation is attempting to quantify the correlation between the AO staining of the thick tissue and slide-mounted specimens as well as the correlation between fluorescence intensity and granularity at the level of an individual cell.
- The stain appears to perform significantly better in fresh tissue than in fixed. This is highly encouraging for the intended purpose but made it difficult to draw definitive conclusions as only one fresh mast cell tumor has been analyzed so far.
- This method could also be used by pathologists to provide a more complete margin assessment than is typically assessed with radial section sampling.
- A much larger sample size of fresh tumors is needed to determine if this method and associated digital analyses can predict the grade. Grading is a challenging task but this study has identified multiple relevant, measurable parameters that may eventually provide clues and thus warrant investigation.
- Future staining modifications and image processing techniques will also attempt to find a solution to the pervasive problem created by the inability to distinguish neoplastic mast cells near the tumor margins from healthy mast cells being called in via inflammatory cytokines.

Acknowledgements

We would like to sincerely thank the UC Davis School of Veterinary Medicine Center for Companion Animal Health Endowment Fund, and the UC Davis SVM STAR program for providing funding support for this project.

Special thanks to Dr. Jennifer Willcox, Dr. Matthew Scheley, Dr. Sarah Stevens, Dr. Phillip Kass, Dr. Anna Massie, Austin Todd, Barbara Zhao, Helena Kons, Michelle Kolb, Dr. Andrea Davis, Dr. Glenn Griffin, Yeonji Cho, all participants who provided data for the visual stain assessment.

References

1. Sledge, D. G., Webster, J. & Kiupel, M. Canine cutaneous mast cell tumors: A combined clinical and pathologic approach to diagnosis, prognosis, and treatment selection. *Vet. J.* **215,** 43–54 (2016).
2. Séguin, B. *et al.* Recurrence rate, clinical outcome, and cellular proliferation indices as prognostic indicators after incomplete surgical excision of cutaneous grade II mast cell tumors: 28 dogs (1994-2002). *J. Vet. Intern. Med.* **20,** 933–940 (2006).
3. Donnelly, L. *et al.* Evaluation of histological grade and histologically tumour-free margins as predictors of local recurrence in completely excised canine mast cell tumours. *Vet. Comp. Oncol.* **13,** 70–76 (2015).
4. Milovancev, M. *et al.* Shaved margin histopathology and imprint cytology for assessment of excision in canine mast cell tumors and soft tissue sarcomas. *Vet. Surg.* **46,** 879–885 (2017).
5. Barthoff DeWitt, S. *et al.* A Novel Imaging System Distinguishes Neoplastic from Normal Tissue During Resection of Soft Tissue Sarcomas and Mast Cell Tumors in Dogs. *Vet. Surg.* **45,** 715–722 (2016).
6. Kiupel, M. *et al.* Proposal of a 2-tier histologic grading system for canine cutaneous mast cell tumors to more accurately predict biological behavior. *Vet. Pathol.* **48,** 147–155 (2011).
7. Zachrisson, B. U. Mast cells of the human gingiva. 2. Metachromatic cells at low pH in healthy and inflamed tissue. *J. Periodontol Res.* **2,** 87–105 (1967).
8. QuPath: Open source software for digital pathology image analysis. Peter Bankhead, Maurice B Loughrey, José A Fernández, Yvonne Dombrowski, Darragh G McArt, Philip D Dunne, Stephen McQuaid, Ronan T Gray
9. Schneider, C. A.; Rasband, W. S. & Eliceiri, K. W. (2012), "NIH Image to ImageJ: 25 years of image analysis", *Nature methods* 9(7): 671-675, PMID 22930834

Note: The colors in figures 6, 7, 9, 11 and 12 have been automatically white balanced for display purposes.